Measurements of Normalized Differential Cross Sections of Inclusive π^0 and K^0_S Production in e^+e^- Annihilation at Energies from 2.2324 to 3.6710 GeV: Supplemental Material

M. Ablikim[1], M. N. Achasov[12,b], P. Adlarson[72], M. Albrecht[4], R. Aliberti[33], A. Amoroso[71A,71C], M. R. An[37], Q. An[68,55], Y. Bai[54], O. Bakina[34], R. Baldini Ferroli[27A], I. Balossino[28A], Y. Ban[44,g], V. Batozskaya[1,42], D. Becker[33], K. Begzsuren[30], N. Berger[33], M. Bertani[27A], D. Bettoni[28A], F. Bianchi[71A,71C], E. Bianco[71A,71C], J. Bloms[65], A. Bortone[71A,71C], I. Boyko[34], R. A. Briere[5], A. Brueggemann[65], H. Cai[73], X. Cai[1,55], A. Calcaterra[27A], G. F. Cao[1,60], N. Cao[1,60], S. A. Cetin[59A], J. F. Chang[1,55], W. L. Chang[1,60], G. R. Che[41], G. Chelkov[34,a], C. Chen[41], Chao Chen[52], G. Chen[1], H. S. Chen[1,60], M. L. Chen[1,55], S. J. Chen[40], S. M. Chen[58], T. Chen[1,60], X. R. Chen[29,60], X. T. Chen[1,60], Y. B. Chen[1,55], Z. J. Chen[24,h], W. S. Cheng[71C], S. K. Choi [52], X. Chu[41], G. Cibinetto[28A], F. Cossio[71C], J. J. Cui[47], H. L. Dai[1,55], J. P. Dai[76], A. Dbeyssi[18], R. E. de Boer[4], D. Dedovich[34], Z. Y. Deng[1], A. Denig[33], I. Denysenko[34], M. Destefanis[71A,71C], F. De Mori[71A,71C], Y. Ding[38], Y. Ding[32], J. Dong[1,55], L. Y. Dong[1,60], M. Y. Dong[1,55,60], X. Dong[73], S. X. Du[78], Z. H. Duan[40], P. Egorov[34,a], Y. L. Fan[73], J. Fang[1,55], S. S. Fang[1,60], W. X. Fang[1], Y. Fang[1], R. Farinelli[28A], L. Fava[71B,71C], F. Feldbauer[4], G. Felici[27A], C. Q. Feng[68,55], J. H. Feng[56], K Fischer[66], M. Fritsch[4], C. Fritzsch[65], C. D. Fu[1], H. Gao[60], X. L. Gao[68,m], Y. N. Gao[44,g], Yang Gao[68,55], S. Garbolino[71C], I. Garzia[28A,28B], P. T. Ge[73], Z. W. Ge[40], C. Geng[56], E. M. Gersabeck[64], A Gilman[66], K. Goetzen[13], L. Gong[38], W. X. Gong[1,55], W. Gradl[33], M. Greco[71A,71C], L. M. Gu[40], M. H. Gu[1,55], Y. T. Gu[15], C. Y Guan[1,60], A. Q. Guo[29,60], L. B. Guo[39], R. P. Guo[46], Y. P. Guo[11,f], A. Guskov[34,a], W. Y. Han[37], X. Q. Hao[19], F. A. Harris[62], K. K. He[52], K. L. He[1,60], F. H. Heinsius[4], C. H. Heinz[33], Y. K. Heng[1,55,60], C. Herold[57], G. Y. Hou[1,60], Y. R. Hou[60], Z. L. Hou[1], H. M. Hu[1,60], J. F. Hu[53,i], T. Hu[1,55,60], Y. Hu[1], G. S. Huang[68,55], K. X. Huang[56], L. Q. Huang[29,60], X. T. Huang[47], Y. P. Huang[1], Z. Huang[44,g], T. Hussain[70], N. Hüsken[26,33], W. Imoehl[26], M. Irshad[68,55], J. Jackson[26], S. Jaeger[4], S. Janchiv[30], E. Jang[52], J. H. Jeong[52], Q. Ji[1], Q. P. Ji[19], X. B. Ji[1,60], X. L. Ji[1,55], Y. Y. Ji[47], Z. K. Jia[68,55], P. C. Jiang[44,g], S. S. Jiang[37], X. S. Jiang[1,55,60], Y. Jiang[60], J. B. Jiao[47], Z. Jiao[22], S. Jin[40], Y. Jin[63], M. Q. Jing[1,60], T. Johansson[72], S. Kabana[31], N. Kalantar-Nayestanaki[61], X. L. Kang[9], X. S. Kang[38], R. Kappert[61], M. Kavatsyuk[61], B. C. Ke[78], I. K. Keshk[4], A. Khoukaz[65], R. Kiuchi[1], R. Kliemt[13], L. Koch[35], O. B. Kolcu[59A], B. Kopf[4], M. Kuemmel[4], M. Kuessner[4], A. Kupsc[42,72], W. Kühn[35], J. J. Lane[64], J. S. Lange[35], P. Larin[18], A. Lavania[25], L. Lavezzi[71A,71C], T. T. Lei[68,k], Z. H. Lei[68,55], H. Leithoff[33], M. Lellmann[33], T. Lenz[33], C. Li[41], C. Li[45], C. H. Li[37], Cheng Li[68,55], D. M. Li[78], F. Li[1,55], G. Li[1], H. Li[49], H. Li[68,55], H. B. Li[1,60], H. J. Li[19], H. N. Li[53,i], J. Q. Li[4], J. S. Li[56], J. W. Li[47], Ke Li[1], L. J Li[1,60], L. K. Li[1], Lei Li[3], M. H. Li[41], P. R. Li[36,j,k], S. X. Li[11], S. Y. Li[58], T. Li[47], W. D. Li[1,60], W. G. Li[1], X. H. Li[68,55], X. L. Li[47], Xiaoyu Li[1,60], Y. G. Li[44,g], Z. X. Li[15], Z. Y. Li[56], C. Liang[40], H. Liang[32], H. Liang[1,60], H. Liang[68,55], Y. F. Liang[51], Y. T. Liang[29,60], G. R. Liao[14], L. Z. Liao[47], J. Libby[25], A. Limphirat[57], C. X. Lin[56], D. X. Lin[29,60], T. Lin[1], B. J. Liu[1], C. Liu[32], C. X. Liu[1], D. Liu[18,68], F. H. Liu[50], Fang Liu[1], Feng Liu[6], G. M. Liu[53,i], H. Liu[36,j,k], H. B. Liu[15], H. M. Liu[1,60], Huanhuan Liu[1], Huihui Liu[20], J. B. Liu[68,55], J. L. Liu[69], J. Y. Liu[1,60], K. Liu[1], K. Y. Liu[38], Ke Liu[21], L. Liu[68,55], Lu Liu[41], M. H. Liu[11,f], P. L. Liu[1], Q. Liu[60], S. B. Liu[68,55], T. Liu[11,f], W. K. Liu[41], W. M. Liu[68,55], X. Liu[36,j,k], Y. Liu[36,j,k], Y. B. Liu[41], Z. A. Liu[1,55,60], Z. Q. Liu[47], X. C. Lou[1,55,60], F. X. Lu[56], H. J. Lu[22], J. G. Lu[1,55], X. L. Lu[1], Y. Lu[7], Y. P. Lu[1,55], Z. H. Lu[1,60], C. L. Luo[39], M. X. Luo[77], T. Luo[11,f], X. L. Luo[1,55], X. R. Lyu[60], Y. F. Lyu[41], F. C. Ma[38], H. L. Ma[1], L. L. Ma[47], M. M. Ma[1,60], Q. M. Ma[1], R. Q. Ma[1,60], R. T. Ma[60], X. Y. Ma[1,55], Y. Ma[44,g], F. E. Maas[18], M. Maggiora[71A,71C], S. Maldaner[4], S. Malde[66], Q. A. Malik[70], A. Mangoni[27B], Y. J. Mao[44,g], Z. P. Mao[1], S. Marcello[71A,71C], Z. X. Meng[63], J. G. Messchendorp[13,61], G. Mezzadri[28A], H. Miao[1,60], T. J. Min[40], R. E. Mitchell[26], X. H. Mo[1,55,60], N. Yu. Muchnoi[12,b], Y. Nefedov[34], F. Nerling[18,d], I. B. Nikolaev[12,b], Z. Ning[1,55], S. Nisar[10,l], Y. Niu [47], S. L. Olsen[60], Q. Ouyang[1,55,60], S. Pacetti[27B,27C], X. Pan[11,f], Y. Pan[54], A. Pathak[32], Y. P. Pei[68,55], M. Pelizaeus[4], H. P. Peng[68,55], K. Peters[13,d], J. L. Ping[39], R. G. Ping[1,60], S. Plura[33], S. Pogodin[34], V. Prasad[68,55], F. Z. Qi[1], H. Qi[68,55], H. R. Qi[58], M. Qi[40], T. Y. Qi[11,f], S. Qian[1,55], W. B. Qian[60], Z. Qian[56], C. F. Qiao[60], J. J. Qin[69], L. Q. Qin[14], X. P. Qin[11,f], X. S. Qin[47], Z. H. Qin[1,55], J. F. Qiu[1], S. Q. Qu[58], K. H. Rashid[70], C. F. Redmer[33], K. J. Ren[37], A. Rivetti[71C], V. Rodin[61], M. Rolo[71C], G. Rong[1,60], Ch. Rosner[18], S. N. Ruan[41], A. Sarantsev[34,c], Y. Schelhaas[33], C. Schnier[4], K. Schoenning[72], M. Scodeggio[28A,28B], K. Y. Shan[11,f], W. Shan[23], X. Y. Shan[68,55], J. F. Shangguan[52], L. G. Shao[1,60], M. Shao[68,55], C. P. Shen[11,f], H. F. Shen[1,60], W. H. Shen[60], X. Y. Shen[1,60], B. A. Shi[60], H. C. Shi[68,55], J. Y. Shi[1], Q. Q. Shi[52], R. S. Shi[1,60], X. Shi[1,55], J. J. Song[19], W. M. Song[32,1], Y. X. Song[44,g], S. Sosio[71A,71C], S. Spataro[71A,71C], F. Stieler[33], P. P. Su[52], Y. J. Su[60], G. X. Sun[1], H. Sun[60], H. K. Sun[1], J. F. Sun[19], L. Sun[73], S. S. Sun[1,60], T. Sun[1,60], W. Y. Sun[32], Y. J. Sun[68,55], Y. Z. Sun[1], Z. T. Sun[47], Y. H. Tan[73], Y. X. Tan[68,55], C. J. Tang[51], G. Y. Tang[1], J. Tang[56], L. Y Tao[69], Q. T. Tao[24,h], M. Tat[66], J. X. Teng[68,55], V. Thoren[72], W. H. Tian[49], Y. Tian[29,60], I. Uman[59B], B. Wang[68,55], B. Wang[1], B. L. Wang[60], C. W. Wang[40], D. Y. Wang[44,g], F. Wang[69], H. J. Wang[36,j,k], H. P. Wang[1,60], K. Wang[1,55], L. L. Wang[1], M. Wang[47], M. Z. Wang[44,g], Meng Wang[1,60], S. Wang[11,f], S. Wang[14], T. Wang[11,f], T. J. Wang[41], W. Wang[56], W. H. Wang[73], W. P. Wang[68,55], X. Wang[44,g], X. F. Wang[36,j,k], X. L. Wang[11,f], Y. Wang[58], Y. D. Wang[43], Y. F. Wang[1,55,60], Y. H. Wang[45], Y. Q. Wang[1], Yaqian Wang[17,1], Z. Wang[1,55], Z. Y. Wang[1,60], Ziyi Wang[60], D. H. Wei[14], F. Weidner[65], S. P. Wen[1], D. J. White[64], U. Wiedner[4], G. Wilkinson[66], M. Wolke[72], L. Wollenberg[4], J. F. Wu[1,60], L. H. Wu[1], L. J. Wu[1,60], X. Wu[11,f], X. H. Wu[32], Y. Wu[68], Y. J Wu[29], Z. Wu[1,55], L. Xia[68,55], T. Xiang[44,g], D. Xiao[36,j,k], G. Y. Xiao[40], H. Xiao[11,f], S. Y. Xiao[1], Y. L. Xiao[11,f], Z. J. Xiao[39], C. Xie[40], X. H. Xie[44,g], Y. Xie[47], Y. G. Xie[1,55], Y. H. Xie[6], Z. P. Xie[68,55], T. Y. Xing[1,60], C. F. Xu[1,60], C. J. Xu[56], G. F. Xu[1], H. Y. Xu[63], Q. J. Xu[16], X. P. Xu[52], Y. C. Xu[75], Z. P. Xu[40], F. Yan[11,f], L. Yan[11,f], W. B. Yan[68,55], W. C. Yan[78], H. J. Yang[48,e], H. L. Yang[32], H. X. Yang[1], Tao Yang[1], Y. F. Yang[41], Y. X. Yang[1,60], Yifan Yang[1,60], M. Ye[1,55], M. H. Ye[8], J. H. Yin[1], Z. Y. You[56], B. X. Yu[1,55,60], C. X. Yu[41], G. Yu[1,60], T. Yu[69], X. D. Yu[44,g], C. Z. Yuan[1,60], L. Yuan[2], S. C. Yuan[1], X. Q. Yuan[1], Y. Yuan[1,60], Z. Y. Yuan[56], C. X. Yue[37],

A. A. Zafar[70], F. R. Zeng[47], X. Zeng[6], Y. Zeng[24,h], X. Y. Zhai[32], Y. H. Zhan[56], A. Q. Zhang[1,60], B. L. Zhang[1,60], B. X. Zhang[1], D. H. Zhang[41], G. Y. Zhang[19], H. Zhang[68], H. H. Zhang[56], H. H. Zhang[32], H. Q. Zhang[1,55,60], H. Y. Zhang[1,55], J. L. Zhang[74], J. Q. Zhang[39], J. W. Zhang[1,55,60], J. X. Zhang[36,j,k], J. Y. Zhang[1], J. Z. Zhang[1,60], Jianyu Zhang[1,60], Jiawei Zhang[1,60], L. M. Zhang[58], L. Q. Zhang[56], Lei Zhang[40], P. Zhang[1], Q. Y. Zhang[37,78], Shuihan Zhang[1,60], Shulei Zhang[24,h], X. D. Zhang[43], X. M. Zhang[1], X. Y. Zhang[47], X. Y. Zhang[52], Y. Zhang[66], Y. T. Zhang[78], Y. H. Zhang[1,55], Yan Zhang[68,55], Yao Zhang[1], Z. H. Zhang[1], Z. L. Zhang[32], Z. Y. Zhang[41], Z. Y. Zhang[73], G. Zhao[1], J. Zhao[37], J. Y. Zhao[1,60], J. Z. Zhao[1,55], Lei Zhao[68,55], Ling Zhao[1], M. G. Zhao[41], S. J. Zhao[78], Y. B. Zhao[1,55], Y. X. Zhao[29,60], Z. G. Zhao[68,55], A. Zhemchugov[34,a], B. Zheng[69], J. P. Zheng[1,55], Y. H. Zheng[60], B. Zhong[39], C. Zhong[69], X. Zhong[56], H. Zhou[47], L. P. Zhou[1,60], X. Zhou[73], X. K. Zhou[60], X. R. Zhou[68,55], X. Y. Zhou[37], Y. Z. Zhou[11,f], J. Zhu[41], K. Zhu[1], K. J. Zhu[1,55,60], L. X. Zhu[60], S. H. Zhu[67], S. Q. Zhu[40], T. J. Zhu[74], W. J. Zhu[11,f], Y. C. Zhu[68,55], Z. A. Zhu[1,60], J. H. Zou[1], J. Zu[68,55]

(BESIII Collaboration)

[1] *Institute of High Energy Physics, Beijing 100049, People's Republic of China*
[2] *Beihang University, Beijing 100191, People's Republic of China*
[3] *Beijing Institute of Petrochemical Technology, Beijing 102617, People's Republic of China*
[4] *Bochum Ruhr-University, D-44780 Bochum, Germany*
[5] *Carnegie Mellon University, Pittsburgh, Pennsylvania 15213, USA*
[6] *Central China Normal University, Wuhan 430079, People's Republic of China*
[7] *Central South University, Changsha 410083, People's Republic of China*
[8] *China Center of Advanced Science and Technology, Beijing 100190, People's Republic of China*
[9] *China University of Geosciences, Wuhan 430074, People's Republic of China*
[10] *COMSATS University Islamabad, Lahore Campus, Defence Road, Off Raiwind Road, 54000 Lahore, Pakistan*
[11] *Fudan University, Shanghai 200433, People's Republic of China*
[12] *G.I. Budker Institute of Nuclear Physics SB RAS (BINP), Novosibirsk 630090, Russia*
[13] *GSI Helmholtzcentre for Heavy Ion Research GmbH, D-64291 Darmstadt, Germany*
[14] *Guangxi Normal University, Guilin 541004, People's Republic of China*
[15] *Guangxi University, Nanning 530004, People's Republic of China*
[16] *Hangzhou Normal University, Hangzhou 310036, People's Republic of China*
[17] *Hebei University, Baoding 071002, People's Republic of China*
[18] *Helmholtz Institute Mainz, Staudinger Weg 18, D-55099 Mainz, Germany*
[19] *Henan Normal University, Xinxiang 453007, People's Republic of China*
[20] *Henan University of Science and Technology, Luoyang 471003, People's Republic of China*
[21] *Henan University of Technology, Zhengzhou 450001, People's Republic of China*
[22] *Huangshan College, Huangshan 245000, People's Republic of China*
[23] *Hunan Normal University, Changsha 410081, People's Republic of China*
[24] *Hunan University, Changsha 410082, People's Republic of China*
[25] *Indian Institute of Technology Madras, Chennai 600036, India*
[26] *Indiana University, Bloomington, Indiana 47405, USA*
[27] *INFN Laboratori Nazionali di Frascati , (A)INFN Laboratori Nazionali di Frascati, I-00044, Frascati, Italy; (B)INFN Sezione di Perugia, I-06100, Perugia, Italy; (C)University of Perugia, I-06100, Perugia, Italy*
[28] *INFN Sezione di Ferrara, (A)INFN Sezione di Ferrara, I-44122, Ferrara, Italy; (B)University of Ferrara, I-44122, Ferrara, Italy*
[29] *Institute of Modern Physics, Lanzhou 730000, People's Republic of China*
[30] *Institute of Physics and Technology, Peace Avenue 54B, Ulaanbaatar 13330, Mongolia*
[31] *Instituto de Alta Investigacion, Universidad de Tarapaca, Casilla 7D, Arica, Chile*
[32] *Jilin University, Changchun 130012, People's Republic of China*
[33] *Johannes Gutenberg University of Mainz, Johann-Joachim-Becher-Weg 45, D-55099 Mainz, Germany*
[34] *Joint Institute for Nuclear Research, 141980 Dubna, Moscow region, Russia*
[35] *Justus-Liebig-Universitaet Giessen, II. Physikalisches Institut, Heinrich-Buff-Ring 16, D-35392 Giessen, Germany*
[36] *Lanzhou University, Lanzhou 730000, People's Republic of China*
[37] *Liaoning Normal University, Dalian 116029, People's Republic of China*
[38] *Liaoning University, Shenyang 110036, People's Republic of China*
[39] *Nanjing Normal University, Nanjing 210023, People's Republic of China*
[40] *Nanjing University, Nanjing 210093, People's Republic of China*
[41] *Nankai University, Tianjin 300071, People's Republic of China*
[42] *National Centre for Nuclear Research, Warsaw 02-093, Poland*
[43] *North China Electric Power University, Beijing 102206, People's Republic of China*
[44] *Peking University, Beijing 100871, People's Republic of China*
[45] *Qufu Normal University, Qufu 273165, People's Republic of China*
[46] *Shandong Normal University, Jinan 250014, People's Republic of China*
[47] *Shandong University, Jinan 250100, People's Republic of China*
[48] *Shanghai Jiao Tong University, Shanghai 200240, People's Republic of China*
[49] *Shanxi Normal University, Linfen 041004, People's Republic of China*

[50] Shanxi University, Taiyuan 030006, People's Republic of China
[51] Sichuan University, Chengdu 610064, People's Republic of China
[52] Soochow University, Suzhou 215006, People's Republic of China
[53] South China Normal University, Guangzhou 510006, People's Republic of China
[54] Southeast University, Nanjing 211100, People's Republic of China
[55] State Key Laboratory of Particle Detection and Electronics, Beijing 100049, Hefei 230026, People's Republic of China
[56] Sun Yat-Sen University, Guangzhou 510275, People's Republic of China
[57] Suranaree University of Technology, University Avenue 111, Nakhon Ratchasima 30000, Thailand
[58] Tsinghua University, Beijing 100084, People's Republic of China
[59] Turkish Accelerator Center Particle Factory Group, (A)Istinye University, 34010, Istanbul, Turkey; (B)Near East University, Nicosia, North Cyprus, Mersin 10, Turkey
[60] University of Chinese Academy of Sciences, Beijing 100049, People's Republic of China
[61] University of Groningen, NL-9747 AA Groningen, The Netherlands
[62] University of Hawaii, Honolulu, Hawaii 96822, USA
[63] University of Jinan, Jinan 250022, People's Republic of China
[64] University of Manchester, Oxford Road, Manchester, M13 9PL, United Kingdom
[65] University of Muenster, Wilhelm-Klemm-Strasse 9, 48149 Muenster, Germany
[66] University of Oxford, Keble Road, Oxford OX13RH, United Kingdom
[67] University of Science and Technology Liaoning, Anshan 114051, People's Republic of China
[68] University of Science and Technology of China, Hefei 230026, People's Republic of China
[69] University of South China, Hengyang 421001, People's Republic of China
[70] University of the Punjab, Lahore-54590, Pakistan
[71] University of Turin and INFN, (A)University of Turin, I-10125, Turin, Italy; (B)University of Eastern Piedmont, I-15121, Alessandria, Italy; (C)INFN, I-10125, Turin, Italy
[72] Uppsala University, Box 516, SE-75120 Uppsala, Sweden
[73] Wuhan University, Wuhan 430072, People's Republic of China
[74] Xinyang Normal University, Xinyang 464000, People's Republic of China
[75] Yantai University, Yantai 264005, People's Republic of China
[76] Yunnan University, Kunming 650500, People's Republic of China
[77] Zhejiang University, Hangzhou 310027, People's Republic of China
[78] Zhengzhou University, Zhengzhou 450001, People's Republic of China

[a] Also at the Moscow Institute of Physics and Technology, Moscow 141700, Russia
[b] Also at the Novosibirsk State University, Novosibirsk, 630090, Russia
[c] Also at the NRC "Kurchatov Institute", PNPI, 188300, Gatchina, Russia
[d] Also at Goethe University Frankfurt, 60323 Frankfurt am Main, Germany
[e] Also at Key Laboratory for Particle Physics, Astrophysics and Cosmology, Ministry of Education; Shanghai Key Laboratory for Particle Physics and Cosmology; Institute of Nuclear and Particle Physics, Shanghai 200240, People's Republic of China
[f] Also at Key Laboratory of Nuclear Physics and Ion-beam Application (MOE) and Institute of Modern Physics, Fudan University, Shanghai 200443, People's Republic of China
[g] Also at State Key Laboratory of Nuclear Physics and Technology, Peking University, Beijing 100871, People's Republic of China
[h] Also at School of Physics and Electronics, Hunan University, Changsha 410082, China
[i] Also at Guangdong Provincial Key Laboratory of Nuclear Science, Institute of Quantum Matter, South China Normal University, Guangzhou 510006, China
[j] Also at Frontiers Science Center for Rare Isotopes, Lanzhou University, Lanzhou 730000, People's Republic of China
[k] Also at Lanzhou Center for Theoretical Physics, Lanzhou University, Lanzhou 730000, People's Republic of China
[l] Also at the Department of Mathematical Sciences, IBA, Karachi , Pakistan
[m] Now at Zhejiang Jiaxing Digital City Laboratory Co., Ltd, Jiaxing 314051, People's Republic of China

(Dated: May 26, 2023)

I. SUMMARY OF THE OBSERVED YIELDS FOR THE $e^+e^- \to \pi^0/K_S^0 + X$ PROCESS

TABLE I. Summary of $N^{\rm obs}_{\pi^0}$ in different momentum ranges at different c.m. energies, where the uncertainties are statistical.

p_{π^0} (GeV/c)	$\sqrt{s}$ = 2.2324 GeV	$\sqrt{s}$ = 2.4000 GeV	$\sqrt{s}$ = 2.8000 GeV	$\sqrt{s}$ = 3.0500 GeV	$\sqrt{s}$ = 3.4000 GeV	$\sqrt{s}$ = 3.6710 GeV
0.00 − 0.10	1790 ± 171	1875 ± 166	1862 ± 49	6184 ± 363	642 ± 121	1296 ± 108
0.10 − 0.20	7894 ± 427	8144 ± 292	7530 ± 282	28454 ± 647	3150 ± 215	7588 ± 118
0.20 − 0.30	11640 ± 222	13428 ± 249	11952 ± 259	41689 ± 502	4470 ± 171	10986 ± 100
0.30 − 0.40	12659 ± 195	14872 ± 255	12872 ± 211	44503 ± 415	5080 ± 161	12117 ± 257
0.40 − 0.50	9690 ± 150	11416 ± 167	10425 ± 174	35120 ± 335	4071 ± 112	9405 ± 167
0.50 − 0.60	6534 ± 114	7776 ± 128	7082 ± 123	25612 ± 235	2954 ± 49	7125 ± 120
0.60 − 0.70	3735 ± 81	4695 ± 101	4598 ± 101	17164 ± 175	2066 ± 67	4975 ± 105
0.70 − 0.80	2135 ± 60	2764 ± 68	3047 ± 75	10830 ± 154	1440 ± 59	3529 ± 94
0.80 − 0.90	1350 ± 43	1596 ± 49	1871 ± 56	7077 ± 116	923 ± 43	2350 ± 71
0.90 − 1.00	949 ± 33	918 ± 34	1143 ± 42	4548 ± 90	545 ± 32	1591 ± 45
1.00 − 1.10	–	634 ± 28	727 ± 32	2884 ± 64	386 ± 24	981 ± 42
1.10 − 1.20	–	–	367 ± 24	1758 ± 56	273 ± 21	674 ± 36
1.20 − 1.30	–	–	269 ± 17	1010 ± 37	186 ± 17	494 ± 30
1.30 − 1.40	–	–	–	494 ± 28	129 ± 10	351 ± 23
1.40 − 1.50	–	–	–	–	69 ± 11	221 ± 15
1.50 − 1.60	–	–	–	–	32 ± 5	114 ± 12
1.60 − 1.70	–	–	–	–	–	59 ± 11

TABLE II. Summary of $N^{\rm obs}_{K_S^0}$ in different momentum ranges at different c.m. energies, where the uncertainties are statistical.

$p_{K_S^0}$ (GeV/c)	$\sqrt{s}$ = 2.2324 GeV	$\sqrt{s}$ = 2.4000 GeV	$\sqrt{s}$ = 2.8000 GeV	$\sqrt{s}$ = 3.0500 GeV	$\sqrt{s}$ = 3.4000 GeV	$\sqrt{s}$ = 3.6710 GeV
0.00 − 0.10	48 ± 7	30 ± 6	27 ± 4	108 ± 13	9 ± 3	29 ± 7
0.10 − 0.20	271 ± 19	327 ± 22	258 ± 18	814 ± 38	68 ± 9	212 ± 17
0.20 − 0.30	501 ± 28	584 ± 30	579 ± 30	1739 ± 52	199 ± 18	371 ± 27
0.30 − 0.40	594 ± 31	743 ± 34	765 ± 35	2375 ± 66	285 ± 21	587 ± 33
0.40 − 0.50	552 ± 33	683 ± 35	721 ± 33	2468 ± 69	264 ± 20	596 ± 34
0.50 − 0.60	390 ± 25	511 ± 30	634 ± 33	2075 ± 62	258 ± 21	557 ± 29
0.60 − 0.70	273 ± 21	363 ± 25	416 ± 25	1613 ± 52	219 ± 17	511 ± 28
0.70 − 0.80	146 ± 15	221 ± 17	323 ± 21	1188 ± 42	149 ± 15	384 ± 24
0.80 − 0.90	137 ± 14	121 ± 14	192 ± 17	875 ± 35	120 ± 13	264 ± 21
0.90 − 1.00	–	128 ± 12	97 ± 12	596 ± 30	64 ± 10	222 ± 17
1.00 − 1.10	–	–	77 ± 10	351 ± 22	44 ± 7	145 ± 14
1.10 − 1.20	–	–	30 ± 6	196 ± 17	48 ± 8	100 ± 12
1.20 − 1.30	–	–	–	82 ± 12	17 ± 4	58 ± 9
1.30 − 1.40	–	–	–	–	16 ± 4	40 ± 8
1.40 − 1.50	–	–	–	–	–	31 ± 5

II. THE p_t ACCEPTANCE OF THE INCLUSIVELY RECONSTRUCTED π^0 AND K_S^0 MESONS

Figure 1 illustrates the coverage of the polar (θ) and azimuthal (ϕ) angles for the π^0 and K_S^0 mesons reconstructed at $\sqrt{s} = 2.8000$ GeV, in which our data have sufficient acceptance in terms of the polar and azimuthal angles and can be reliably reproduced by the signal MC model in reconstruction level.

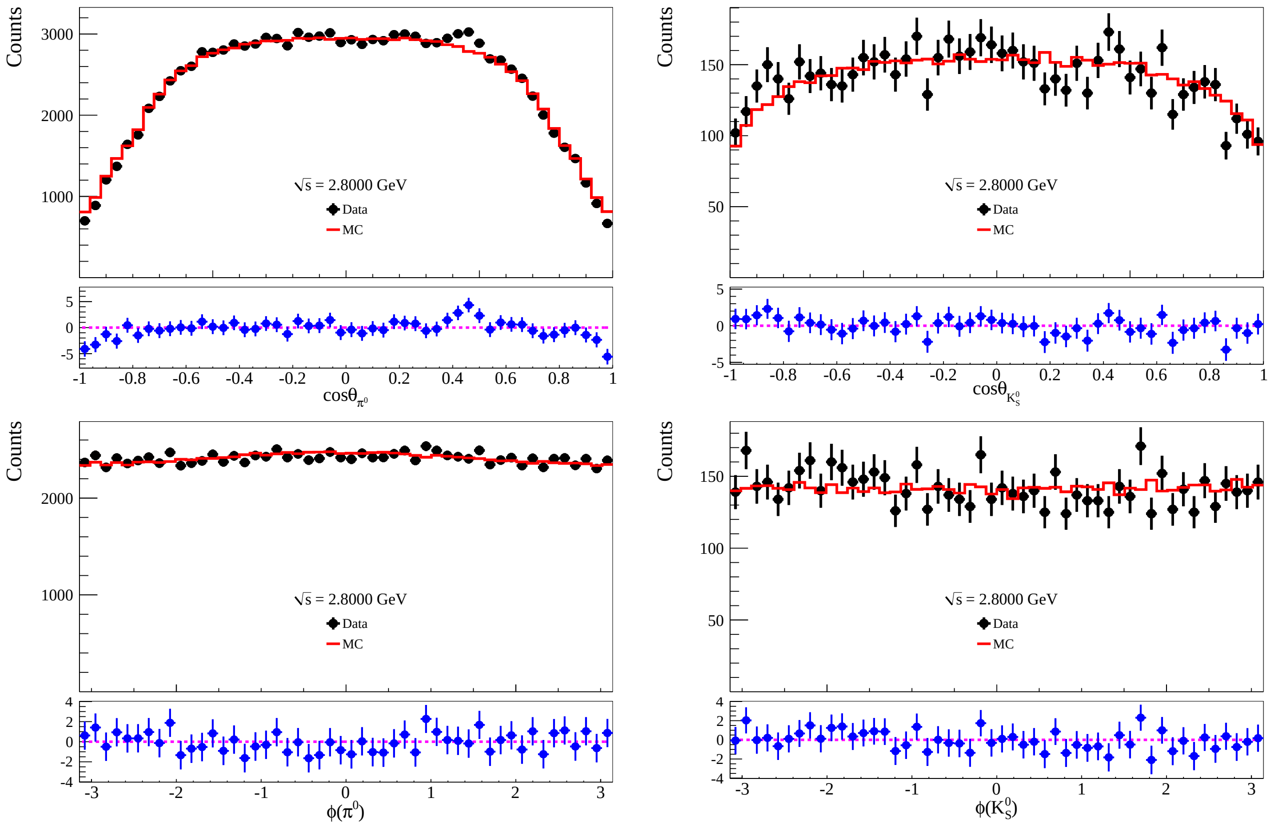

FIG. 1. Comparisons between data and simulation in terms of the $\cos\theta$ (top) and azimuthal angle (ϕ, bottom) distributions of π^0 (left) and K_S^0 (right) at $\sqrt{s} = 2.8000$ GeV, where θ is the polar angle. The black dots represent experimental data and red histograms stand for the signal MC. The blue dots denote the corresponding PULL distributions.

To provide the p_t acceptance information of the inclusively reconstructed π^0 and K^0_S mesons to the future phenomenology study, the two-dimensional distributions of the momentum (p) and transverse momentum (p_t) of π^0 and K^0_S at MC truth and reconstruction level at $\sqrt{s} = 2.8000$ GeV are given in Fig. 2.

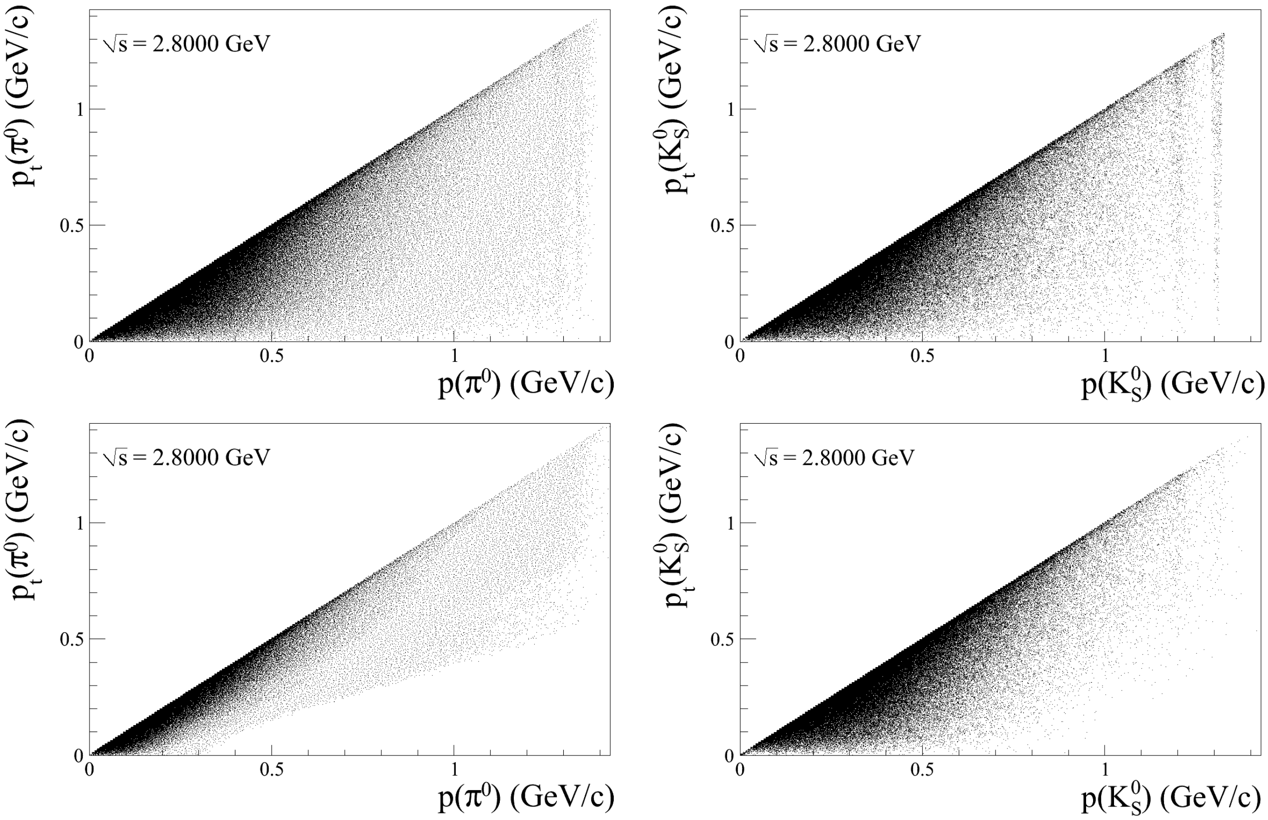

FIG. 2. Two-dimensional distributions of the momentum (p) and transverse momentum (p_t) of π^0 (left) and K^0_S (right) in MC truth (top) and reconstruction level (bottom) at $\sqrt{s} = 2.8000$ GeV. These plots are extracted from the signal MC samples produced by the LUARLW model. The event lost in the low-p_t region after reconstruction is caused by the limited acceptance of the BESIII detector in the small polar angle region and will be compensated by the correction factor f_h of the corresponding momentum bin in the analysis.

III. SUMMARY OF THE CORRECTION FACTORS FOR THE $e^+e^- \to \pi^0/K_S^0 + X$ PROCESS

TABLE III. Summary of f_{π^0} for different momentum ranges at different c.m. energies, where the first uncertainty is statistical and second is systematical due to the signal simulation model.

p_{π^0} (GeV/c)	$\sqrt{s}$ = 2.2324 GeV	$\sqrt{s}$ = 2.4000 GeV	$\sqrt{s}$ = 2.8000 GeV	$\sqrt{s}$ = 3.0500 GeV	$\sqrt{s}$ = 3.4000 GeV	$\sqrt{s}$ = 3.6710 GeV
0.00 − 0.10	2.366 ± 0.034 ± 0.140	2.349 ± 0.034 ± 0.190	2.382 ± 0.039 ± 0.134	2.389 ± 0.042 ± 0.275	2.609 ± 0.048 ± 0.294	2.555 ± 0.051 ± 0.048
0.10 − 0.20	2.328 ± 0.016 ± 0.106	2.403 ± 0.018 ± 0.064	2.454 ± 0.019 ± 0.032	2.577 ± 0.021 ± 0.162	2.776 ± 0.023 ± 0.016	2.708 ± 0.023 ± 0.189
0.20 − 0.30	2.160 ± 0.010 ± 0.057	2.197 ± 0.011 ± 0.025	2.280 ± 0.012 ± 0.011	2.372 ± 0.012 ± 0.012	2.561 ± 0.014 ± 0.006	2.497 ± 0.013 ± 0.067
0.30 − 0.40	1.818 ± 0.007 ± 0.039	1.866 ± 0.007 ± 0.013	1.964 ± 0.007 ± 0.023	2.030 ± 0.008 ± 0.059	2.215 ± 0.009 ± 0.104	2.188 ± 0.010 ± 0.050
0.40 − 0.50	1.743 ± 0.006 ± 0.006	1.799 ± 0.007 ± 0.006	1.887 ± 0.007 ± 0.052	1.941 ± 0.008 ± 0.055	2.080 ± 0.009 ± 0.087	2.096 ± 0.009 ± 0.044
0.50 − 0.60	1.741 ± 0.008 ± 0.010	1.770 ± 0.007 ± 0.021	1.849 ± 0.008 ± 0.051	1.907 ± 0.008 ± 0.014	1.961 ± 0.009 ± 0.023	2.028 ± 0.010 ± 0.029
0.60 − 0.70	1.741 ± 0.009 ± 0.018	1.788 ± 0.009 ± 0.014	1.821 ± 0.009 ± 0.117	1.872 ± 0.005 ± 0.078	1.874 ± 0.010 ± 0.084	1.964 ± 0.011 ± 0.035
0.70 − 0.80	1.813 ± 0.012 ± 0.004	1.815 ± 0.011 ± 0.041	1.856 ± 0.010 ± 0.146	1.882 ± 0.011 ± 0.171	1.786 ± 0.011 ± 0.211	1.912 ± 0.013 ± 0.128
0.80 − 0.90	1.985 ± 0.016 ± 0.101	1.923 ± 0.014 ± 0.061	1.916 ± 0.013 ± 0.179	1.934 ± 0.013 ± 0.189	1.795 ± 0.012 ± 0.252	1.918 ± 0.014 ± 0.166
0.90 − 1.00	2.295 ± 0.022 ± 0.262	2.124 ± 0.020 ± 0.278	2.031 ± 0.016 ± 0.210	1.987 ± 0.015 ± 0.276	1.812 ± 0.014 ± 0.306	1.906 ± 0.016 ± 0.274
1.00 − 1.10	−	2.454 ± 0.027 ± 0.523	2.138 ± 0.021 ± 0.223	2.042 ± 0.017 ± 0.359	1.855 ± 0.016 ± 0.322	1.926 ± 0.017 ± 0.451
1.10 − 1.20	−	−	2.354 ± 0.026 ± 0.410	2.168 ± 0.024 ± 0.365	1.967 ± 0.022 ± 0.284	1.951 ± 0.019 ± 0.415
1.20 − 1.30	−	−	2.637 ± 0.039 ± 1.292	2.458 ± 0.033 ± 0.587	2.092 ± 0.023 ± 0.465	2.069 ± 0.023 ± 0.491
1.30 − 1.40	−	−	−	2.451 ± 0.042 ± 1.015	2.223 ± 0.028 ± 0.517	2.064 ± 0.024 ± 0.669
1.40 − 1.50	−	−	−	−	2.457 ± 0.039 ± 0.724	2.241 ± 0.030 ± 0.903
1.50 − 1.60	−	−	−	−	2.846 ± 0.058 ± 1.100	2.478 ± 0.039 ± 0.758
1.60 − 1.70	−	−	−	−	−	2.788 ± 0.036 ± 1.758

TABLE IV. Summary of $f_{K_S^0}$ for different momentum ranges at different c.m. energies, where the first uncertainty is statistical and second is systematical due to the signal simulation model.

$p_{K_S^0}$ (GeV/c)	$\sqrt{s}$ = 2.2324 GeV	$\sqrt{s}$ = 2.4000 GeV	$\sqrt{s}$ = 2.8000 GeV	$\sqrt{s}$ = 3.0500 GeV	$\sqrt{s}$ = 3.4000 GeV	$\sqrt{s}$ = 3.6710 GeV
0.00 − 0.10	4.207 ± 0.108 ± 0.300	3.952 ± 0.108 ± 0.143	3.938 ± 0.096 ± 0.184	4.200 ± 0.101 ± 0.213	4.482 ± 0.136 ± 0.973	4.093 ± 0.095 ± 0.110
0.10 − 0.20	3.228 ± 0.038 ± 0.198	3.264 ± 0.038 ± 0.211	3.117 ± 0.035 ± 0.225	3.183 ± 0.034 ± 0.163	3.564 ± 0.051 ± 0.807	3.353 ± 0.038 ± 0.226
0.20 − 0.30	2.903 ± 0.038 ± 0.047	3.026 ± 0.030 ± 0.192	2.933 ± 0.026 ± 0.055	2.922 ± 0.027 ± 0.261	3.278 ± 0.034 ± 0.559	3.174 ± 0.029 ± 0.366
0.30 − 0.40	2.888 ± 0.034 ± 0.221	2.925 ± 0.030 ± 0.355	2.828 ± 0.023 ± 0.014	2.836 ± 0.024 ± 0.209	3.150 ± 0.033 ± 0.530	2.917 ± 0.030 ± 0.452
0.40 − 0.50	2.871 ± 0.051 ± 0.390	2.951 ± 0.047 ± 0.263	2.876 ± 0.030 ± 0.072	2.751 ± 0.027 ± 0.034	3.005 ± 0.042 ± 0.406	2.910 ± 0.036 ± 0.466
0.50 − 0.60	3.271 ± 0.071 ± 0.007	3.106 ± 0.045 ± 0.298	2.897 ± 0.041 ± 0.368	2.758 ± 0.047 ± 0.133	3.071 ± 0.040 ± 0.287	2.814 ± 0.055 ± 0.408
0.60 − 0.70	3.326 ± 0.073 ± 0.477	3.333 ± 0.086 ± 0.127	2.906 ± 0.051 ± 0.072	2.777 ± 0.051 ± 0.230	2.989 ± 0.054 ± 0.175	2.977 ± 0.048 ± 0.448
0.70 − 0.80	4.239 ± 0.121 ± 0.057	3.744 ± 0.106 ± 0.256	3.193 ± 0.056 ± 0.307	2.886 ± 0.050 ± 0.007	3.047 ± 0.050 ± 0.170	2.950 ± 0.048 ± 0.272
0.80 − 0.90	5.604 ± 0.174 ± 0.076	3.998 ± 0.126 ± 0.353	3.222 ± 0.076 ± 0.163	3.205 ± 0.071 ± 0.140	2.947 ± 0.059 ± 0.011	2.971 ± 0.048 ± 0.344
0.90 − 1.00	−	5.324 ± 0.192 ± 0.504	4.054 ± 0.112 ± 0.371	3.152 ± 0.076 ± 0.137	3.038 ± 0.078 ± 0.276	2.897 ± 0.058 ± 0.104
1.00 − 1.10	−	−	4.505 ± 0.170 ± 0.405	3.689 ± 0.115 ± 0.605	3.271 ± 0.084 ± 0.602	2.849 ± 0.068 ± 0.000
1.10 − 1.20	−	−	5.132 ± 0.252 ± 0.456	4.171 ± 0.157 ± 1.024	3.618 ± 0.110 ± 0.867	3.014 ± 0.074 ± 0.158
1.20 − 1.30	−	−	−	4.643 ± 0.281 ± 1.979	3.665 ± 0.183 ± 0.290	3.150 ± 0.094 ± 0.119
1.30 − 1.40	−	−	−	−	3.713 ± 0.261 ± 0.617	3.483 ± 0.124 ± 0.692
1.40 − 1.50	−	−	−	−	−	3.996 ± 0.266 ± 1.155

IV. NORMALIZED DIFFERENTIAL CROSS SECTIONS OF THE $e^+e^- \to \pi^0/K_S^0 + X$ PROCESS

TABLE V. Summary of normalized differential cross sections of the $e^+e^- \to \pi^0 + X$ process at different momentum ranges, where the first uncertainties are statistical and the second are systematic, respectively. Systematic uncertainties are regarded as uncorrelated between different momentum ranges except 2% of that due to the reconstruction of the photons.

p_{π^0} (GeV/c)	$\sqrt{s}$ = 2.2324 GeV	$\sqrt{s}$ = 2.4000 GeV	$\sqrt{s}$ = 2.8000 GeV	$\sqrt{s}$ = 3.0500 GeV	$\sqrt{s}$ = 3.4000 GeV	$\sqrt{s}$ = 3.6710 GeV
0.00 − 0.10	0.522 ± 0.051 ± 0.121	0.467 ± 0.042 ± 0.065	0.543 ± 0.017 ± 0.127	0.535 ± 0.033 ± 0.099	0.534 ± 0.101 ± 0.258	0.482 ± 0.041 ± 0.141
0.10 − 0.20	2.263 ± 0.124 ± 0.213	2.075 ± 0.076 ± 0.211	2.261 ± 0.087 ± 0.390	2.656 ± 0.065 ± 0.203	2.789 ± 0.193 ± 0.306	2.987 ± 0.054 ± 0.577
0.20 − 0.30	3.097 ± 0.062 ± 0.240	3.128 ± 0.061 ± 0.098	3.334 ± 0.075 ± 0.188	3.581 ± 0.048 ± 0.282	3.651 ± 0.142 ± 0.242	3.988 ± 0.045 ± 0.437
0.30 − 0.40	2.834 ± 0.046 ± 0.087	2.943 ± 0.052 ± 0.169	3.093 ± 0.053 ± 0.103	3.272 ± 0.034 ± 0.119	3.588 ± 0.116 ± 0.190	3.854 ± 0.085 ± 0.211
0.40 − 0.50	2.081 ± 0.034 ± 0.046	2.178 ± 0.034 ± 0.048	2.407 ± 0.042 ± 0.086	2.468 ± 0.026 ± 0.086	2.700 ± 0.077 ± 0.150	2.866 ± 0.054 ± 0.087
0.50 − 0.60	1.401 ± 0.026 ± 0.032	1.460 ± 0.025 ± 0.036	1.603 ± 0.029 ± 0.057	1.769 ± 0.018 ± 0.039	1.847 ± 0.033 ± 0.070	2.101 ± 0.038 ± 0.064
0.60 − 0.70	0.801 ± 0.018 ± 0.023	0.890 ± 0.020 ± 0.025	1.024 ± 0.023 ± 0.070	1.164 ± 0.013 ± 0.054	1.234 ± 0.041 ± 0.062	1.420 ± 0.032 ± 0.045
0.70 − 0.80	0.477 ± 0.014 ± 0.014	0.532 ± 0.014 ± 0.019	0.692 ± 0.018 ± 0.063	0.738 ± 0.011 ± 0.069	0.820 ± 0.035 ± 0.100	0.981 ± 0.027 ± 0.071
0.80 − 0.90	0.330 ± 0.011 ± 0.026	0.326 ± 0.010 ± 0.015	0.439 ± 0.014 ± 0.043	0.496 ± 0.009 ± 0.050	0.528 ± 0.025 ± 0.076	0.655 ± 0.020 ± 0.062
0.90 − 1.00	0.268 ± 0.010 ± 0.032	0.207 ± 0.008 ± 0.029	0.284 ± 0.011 ± 0.031	0.327 ± 0.007 ± 0.046	0.315 ± 0.019 ± 0.054	0.441 ± 0.013 ± 0.065
1.00 − 1.10	−	0.165 ± 0.007 ± 0.036	0.190 ± 0.009 ± 0.024	0.213 ± 0.005 ± 0.038	0.228 ± 0.014 ± 0.043	0.275 ± 0.012 ± 0.065
1.10 − 1.20	−	−	0.106 ± 0.007 ± 0.019	0.138 ± 0.005 ± 0.024	0.171 ± 0.013 ± 0.026	0.191 ± 0.010 ± 0.041
1.20 − 1.30	−	−	0.087 ± 0.006 ± 0.043	0.090 ± 0.004 ± 0.022	0.124 ± 0.011 ± 0.028	0.149 ± 0.009 ± 0.036
1.30 − 1.40	−	−	−	0.044 ± 0.003 ± 0.018	0.091 ± 0.007 ± 0.023	0.105 ± 0.007 ± 0.035
1.40 − 1.50	−	−	−	−	0.054 ± 0.009 ± 0.016	0.072 ± 0.005 ± 0.030
1.50 − 1.60	−	−	−	−	0.029 ± 0.005 ± 0.011	0.041 ± 0.004 ± 0.013
1.60 − 1.70	−	−	−	−	−	0.024 ± 0.005 ± 0.015

TABLE VI. Summary of normalized differential cross sections of the $e^+e^- \to K_S^0 + X$ process at different momentum ranges, where the first uncertainties are statistical and the second are systematic, respectively. Systematic uncertainties are regarded as uncorrelated between different momentum ranges.

$p_{K_S^0}$ (GeV/c)	$\sqrt{s}$ = 2.2324 GeV	$\sqrt{s}$ = 2.4000 GeV	$\sqrt{s}$ = 2.8000 GeV	$\sqrt{s}$ = 3.0500 GeV	$\sqrt{s}$ = 3.4000 GeV	$\sqrt{s}$ = 3.6710 GeV
0.00 − 0.10	0.025 ± 0.004 ± 0.003	0.013 ± 0.002 ± 0.001	0.013 ± 0.002 ± 0.001	0.016 ± 0.002 ± 0.002	0.013 ± 0.005 ± 0.003	0.017 ± 0.004 ± 0.001
0.10 − 0.20	0.108 ± 0.007 ± 0.010	0.113 ± 0.008 ± 0.010	0.098 ± 0.007 ± 0.009	0.094 ± 0.004 ± 0.007	0.077 ± 0.011 ± 0.019	0.103 ± 0.008 ± 0.010
0.20 − 0.30	0.179 ± 0.009 ± 0.009	0.187 ± 0.010 ± 0.014	0.208 ± 0.011 ± 0.015	0.184 ± 0.006 ± 0.019	0.208 ± 0.019 ± 0.041	0.171 ± 0.012 ± 0.021
0.30 − 0.40	0.211 ± 0.010 ± 0.018	0.230 ± 0.011 ± 0.029	0.265 ± 0.012 ± 0.007	0.244 ± 0.007 ± 0.021	0.286 ± 0.021 ± 0.049	0.249 ± 0.014 ± 0.041
0.40 − 0.50	0.195 ± 0.010 ± 0.027	0.214 ± 0.011 ± 0.020	0.254 ± 0.012 ± 0.009	0.246 ± 0.007 ± 0.009	0.253 ± 0.019 ± 0.036	0.252 ± 0.015 ± 0.042
0.50 − 0.60	0.157 ± 0.010 ± 0.005	0.168 ± 0.010 ± 0.017	0.225 ± 0.012 ± 0.029	0.207 ± 0.007 ± 0.011	0.252 ± 0.021 ± 0.025	0.228 ± 0.012 ± 0.036
0.60 − 0.70	0.112 ± 0.008 ± 0.017	0.128 ± 0.009 ± 0.007	0.148 ± 0.009 ± 0.006	0.162 ± 0.006 ± 0.014	0.209 ± 0.017 ± 0.019	0.221 ± 0.012 ± 0.034
0.70 − 0.80	0.076 ± 0.008 ± 0.004	0.088 ± 0.007 ± 0.007	0.126 ± 0.009 ± 0.013	0.124 ± 0.005 ± 0.006	0.145 ± 0.015 ± 0.011	0.165 ± 0.010 ± 0.015
0.80 − 0.90	0.095 ± 0.010 ± 0.006	0.051 ± 0.006 ± 0.005	0.076 ± 0.007 ± 0.005	0.102 ± 0.005 ± 0.006	0.113 ± 0.012 ± 0.005	0.114 ± 0.009 ± 0.015
0.90 − 1.00	−	0.072 ± 0.007 ± 0.008	0.048 ± 0.006 ± 0.005	0.068 ± 0.004 ± 0.005	0.062 ± 0.010 ± 0.007	0.093 ± 0.007 ± 0.005
1.00 − 1.10	−	−	0.043 ± 0.006 ± 0.005	0.047 ± 0.003 ± 0.008	0.046 ± 0.008 ± 0.009	0.060 ± 0.006 ± 0.003
1.10 − 1.20	−	−	0.019 ± 0.004 ± 0.002	0.030 ± 0.003 ± 0.007	0.055 ± 0.009 ± 0.014	0.044 ± 0.005 ± 0.003
1.20 − 1.30	−	−	−	0.014 ± 0.002 ± 0.006	0.020 ± 0.005 ± 0.003	0.026 ± 0.004 ± 0.002
1.30 − 1.40	−	−	−	−	0.019 ± 0.005 ± 0.004	0.020 ± 0.004 ± 0.004
1.40 − 1.50	−	−	−	−	−	0.018 ± 0.003 ± 0.005

V. NORMALIZED DIFFERENTIAL CROSS SECTIONS AS FUNCTION OF z

In the main text, the normalized differential cross sections of the $e^+e^- \to \pi^0/K_S^0 + X$ process are given as function of hadron momentum. According to the relation $z \equiv 2\sqrt{p_h^2c^2 + M_h^2c^4}/\sqrt{s}$, these cross sections could be converted to be z-dependent by using:

$$\frac{1}{\sigma(e^+e^- \to \text{hadrons})}\frac{\mathrm{d}\sigma(e^+e^- \to h+X)}{\mathrm{d}z_h} = \frac{\sqrt{s}}{2}\sqrt{1+\frac{M_h^2c^2}{p_h^2}}\frac{1}{\sigma(e^+e^- \to \text{hadrons})}\frac{\mathrm{d}\sigma(e^+e^- \to h+X)}{\mathrm{d}p_h} \tag{1}$$

With the binning scheme adopted in this analysis, there is migration of the signal events between different z bins due to the initial-state radiation which reduces the nominal $\sqrt{s}$. An MC-based study shows that the migration is generally small and below 20% for all the z bins at $\sqrt{s} = 2.8000$ GeV. This migration will be reliably corrected by the f_h factor extracted from the signal MC sample.

The z-dependent cross sections are shown in Fig. 3 and Fig. 4 for the $e^+e^- \to \pi^0 + X$ and $e^+e^- \to K_S^0 + X$ processes, respectively.

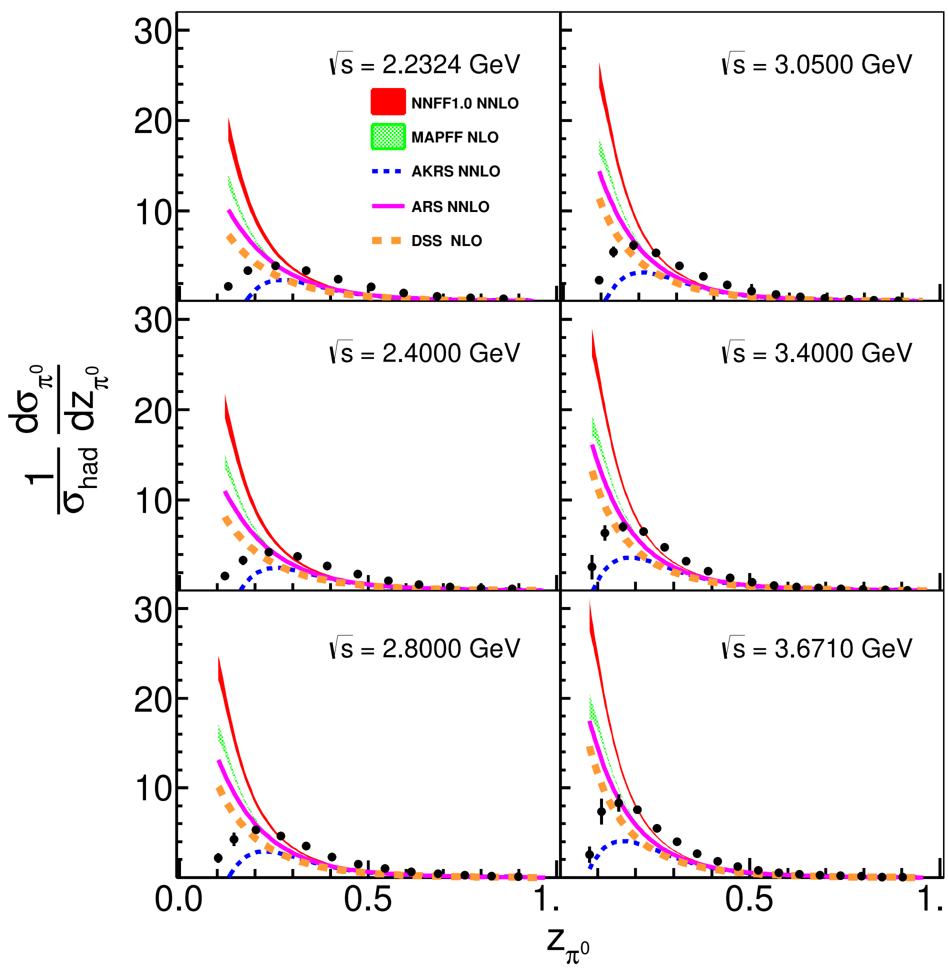

FIG. 3. Normalized differential cross sections of the $e^+e^- \to \pi^0 + X$ process as function of z. The points with error bars are the measured values, where the uncertainties are the quadrature sum of the corresponding statistical and systematic uncertainties. The bands or curves in red, green, blue, magenta, and orange denote the NNFF, MAPFF, AKRS, ARS and DSS calculations, respectively, where only the former two cover $\pm1\sigma$ limits.

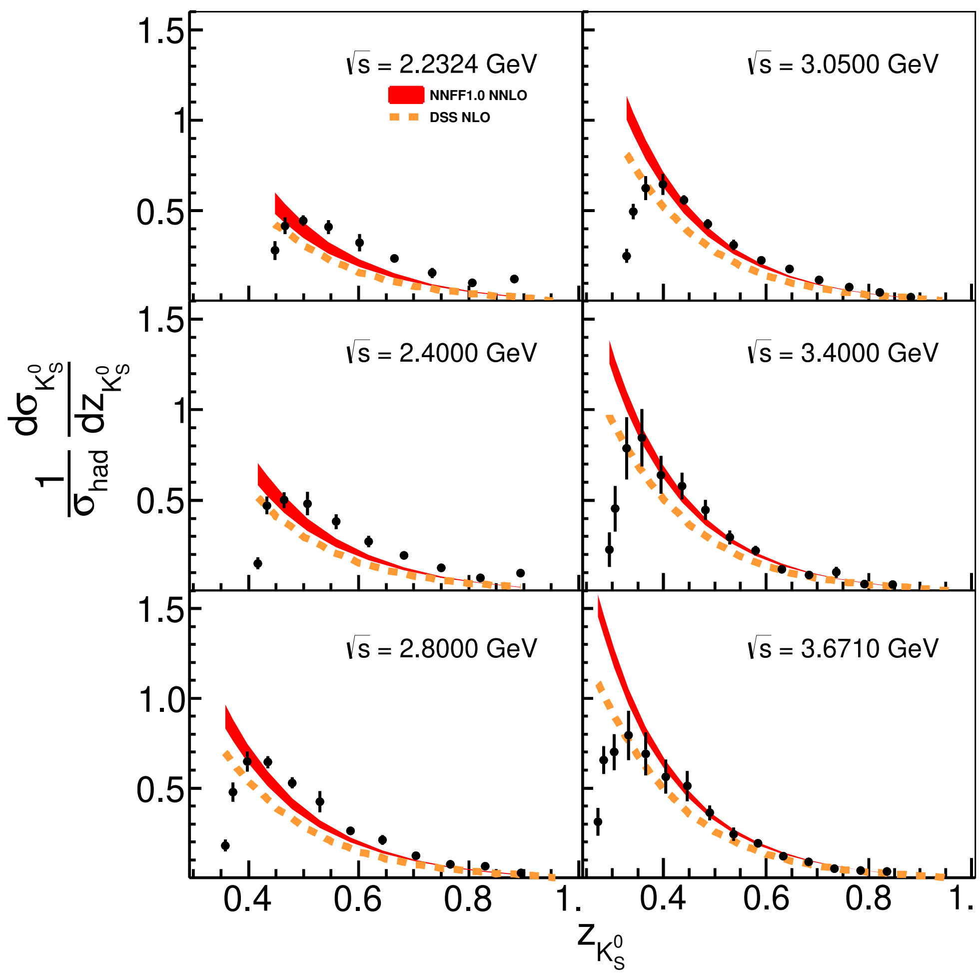

FIG. 4. Normalized differential cross sections of the $e^+e^- \to K_S^0 + X$ process as function of z. The points with error bars are the measured values, where the uncertainties are the quadrature sum of the corresponding statistical and systematic uncertainties. The red band shows the theoretical calculation from NNFF with $\pm 1\sigma$ limits, and the orange curve denotes the prediction of DSS.